THE ASTROPHYSICAL JOURNAL, 276:127–134, 1984 January 1

A GALACTIC DISK AS A TWO-FLUID SYSTEM: CONSEQUENCES FOR THE CRITICAL STELLAR VELOCITY DISPERSION AND THE FORMATION OF CONDENSATIONS IN THE GAS[1]

CHANDA J. JOG[2] AND P. M. SOLOMON[3]
State University of New York at Stony Brook
Received 1983 June 1; accepted 1983 June 13

ABSTRACT

We examine the consequences of treating a galactic disk as a two-fluid system for the stability of the entire disk and for the stability and form of the gas in the disk.

We find that the existence of even a small fraction of the total disk surface density in a cold fluid (that is, the gas) makes it much harder to stabilize the entire two-fluid disk. $(C_{s,\min})_{2\text{-}f}$, the critical stellar velocity dispersion for a two-fluid disk is an increasing function of μ_g/μ_s, the gas fraction, and μ_t/κ, where μ_g, μ_s, and μ_t are the gaseous, stellar, and total disk surface densities and κ is the epicyclic frequency. In the Galaxy, we find that $(C_{s,\min})_{2\text{-}f}$ as a function of R peaks when μ_t/κ peaks—at galactocentric radii of $R \sim 5$–7 kpc; two-fluid instabilities are most likely to occur in this region. This region is coincident with the peak in the molecular cloud distribution in the Galaxy.

At the higher effective gas density resulting from the growth of a two-fluid instability, the gas may become unstable, even when originally the gas by itself is stable. The wavelength of a typical (induced) gas instability in the inner galaxy is ~ 400 pc, and it contains $\sim 10^7\ M_\odot$ of interstellar matter; these instabilities may be identified with clusters of giant molecular clouds.

We suggest that many of the spiral features seen in gas-rich spiral galaxies may be material arms or arm segments resulting from sheared two-fluid gravitational instabilities.

The analysis presented here is applicable to any general disk galaxy consisting of stars and gas.

Subject headings: galaxies: internal motions — galaxies: Milky Way — galaxies: structure — instabilities — interstellar: matter — interstellar: molecules

I. INTRODUCTION

In the preceding paper (Jog and Solomon 1984, hereafter Paper I) we formulated a two-fluid scheme wherein the stars and the gas in a galactic disk are represented as two isothermal fluids, and the two fluids interact gravitationally with each other. The disk is supported by rotation and random motion. We formulated and solved the hydrodynamic equations describing this system and studied the characteristics of the resulting (axisymmetric) two-fluid gravitational instabilities in such a system. The main result from this study was that even when both the fluids in a two-fluid system are separately stable, the joint two-fluid system, due to the gravitational interaction between the two component fluids, may be unstable. Second, the contribution per unit surface density, μ, toward the formation of two-fluid instabilities is substantially greater for the gas than it is for the stars; this is due to the lower gas velocity dispersion C_g as compared to the stellar velocity dispersion C_s.

In this paper, we examine the consequences of treating a galactic disk as a two-fluid system for the stability of the entire disk (§ II) as well as the stability and form of the gas in the disk (§ III). We also comment on the connection between two-fluid instabilities in a disk and the observed small-scale spiral features in external spiral galaxies (§ IV).

In § II we calculate $(C_{s,\min})_{2\text{-}f}$, the critical stellar velocity dispersion needed to stabilize the entire two-fluid disk. For this, we study two-fluid neutral equilibrium. From analytical calculations (for an infinitesimally thin disk) in § II*a*, we find that the ratio of the two-fluid and one-fluid (stars-alone) critical stellar velocity dispersion is always greater than 1 and increases as the gas fraction in the two-fluid disk (at constant total disk surface density) is increased. From the numerical results for a finite height disk presented in § II*b* we find that $(C_{s,\min})_{2\text{-}f}$ is an increasing function of μ_g/μ_s, the ratio of gas to stellar surface densities and μ_t/κ, where μ_t is the total disk surface density and κ is the epicyclic frequency. $(C_{s,\min})_{2\text{-}f}$ as a function of R in the Galaxy peaks at $R = 5$ kpc.

In § III we examine the formation of condensations in the (initially stable) gas as a result of the increase in gas density resulting from the growth of a two-fluid gravitational instability. We find that in the Galaxy, these condensations are most likely to occur at $R = 4$–7 kpc which does indeed coincide with the peak of the molecular ring in the Galaxy. The wavelength of a typical (induced) gas instability in the galactic disk is ~ 400–500 pc, and it contains a mass of gas ~ 1–$2 \times 10^7\ M_\odot$.

Section V contains a summary of the conclusions from this paper.

[1] This paper is based on a dissertation submitted by one of the authors (C. J. Jog) to the State University of New York at Stony Brook in partial fulfillment of the requirements for the Ph.D. degree.

[2] Department of Physics, SUNY, Stony Brook.
[3] Astronomy Program, SUNY, Stony Brook; and Institute of Astronomy, Cambridge, England.

II. DISK STABILITY: TWO-FLUID NEUTRAL EQUILIBRIUM

A one-fluid stellar disk is stable against the growth of axisymmetric perturbations if the (planar one-dimensional rms) stellar velocity dispersion C_s in the disk exceeds the critical stellar velocity dispersion, $(C_{s,\min})_{1\text{-}f}$ $(= \pi G\mu_s/\kappa)$ (Toomre 1964).[4] $(C_{s,\min})_{1\text{-}f}$ corresponds to the neutral equilibrium for a one-fluid disk. We extend Toomre's argument for a neutrally stable one-fluid disk to a disk composed of a two-fluid system and define $(C_{s,\min})_{2\text{-}f}$, the critical stellar velocity dispersion for a two-fluid disk. We solve for $(C_{s,\min})_{2\text{-}f}$ in terms of the other input parameters; this is a valid approach as long as the gas alone is stable.

Recall from § IIc of Paper I that the behavior of a given perturbation mode (k, ω), where $k = (2\pi/\lambda)$ is the wavenumber and ω is the angular frequency, to the two-fluid system (for an infinitesimally thin disk) is governed by:

$$\omega^2(k) = \tfrac{1}{2}\{(\alpha_s + \alpha_g) - [(\alpha_s + \alpha_g)^2 - 4(\alpha_s\alpha_g - \beta_s\beta_g)]^{1/2}\}\,, \quad (1)$$

where

$$\alpha_s = \kappa^2 + k^2C_s^2 - 2\pi Gk\mu_s\,,$$
$$\alpha_g = \kappa^2 + k^2C_g^2 - 2\pi Gk\mu_g\,,$$
$$\beta_s = 2\pi Gk\mu_s\,,$$
$$\beta_g = 2\pi Gk\mu_g\,. \quad (2)$$

The corresponding equations for a finite height two-fluid case are given by equations (23) and (24), respectively (Paper I).

A system is in neutral equilibrium when the following simultaneous equations

$$\omega^2(k) = 0 \quad (3)$$

and

$$d[\omega^2(k)]/dk = 0 \quad (4)$$

have real k solutions.

For the two-fluid system, $\omega^2(k)$ is a fourth order equation in k (see eq. [1]); hence, in this case three solutions for $(k_0)_{2\text{-}f}$, the two-fluid neutral wavenumber, and therefore for $(C_{s,\min})_{2\text{-}f}$—one corresponding to each solution for $(k_0)_{2\text{-}f}$—are possible. We expect $(k_0)_{2\text{-}f}$ to be near the neutral wavenumbers for the stars-alone $(k_0)_s$ and the gas-alone $(k_0)_g$, respectively, for low and high μ_g/μ_s. The resulting solution for $(k_0)_{2\text{-}f}$ in any given case denotes the wavenumber at which it is hardest (or, at which the highest C_s is needed) to stabilize the two-fluid system, by solving for C_s.

a) *Analytical Calculation of* $(C_{s,\min})_{2\text{-}f}$ *for an Infinitesimally Thin Disk*

From the equation for $\omega^2(k)$ for a two-fluid system with zero scale height (eq. [1]), we can see that the condition in equation (3) is identical to

$$\alpha_s\alpha_g - \beta_s\beta_g = 0\,. \quad (5)$$

Equation (5) reduces to (see eqs. [21], [22] in Paper I)

$$\frac{2\pi Gk\mu_s}{\kappa^2 + k^2C_s^2} + \frac{2\pi Gk\mu_g}{\kappa^2 + k^2C_g^2} = 1\,. \quad (6)$$

[4] A hydrodynamic approach yields this definition whereas the distribution function approach used by Toomre gives 3.36 instead of π in the above definition.

Equation (4) reduces to the following form when equation (5) is satisfied:

$$\frac{d}{dk}(\alpha_s\alpha_g - \beta_s\beta_g) = 0\,.$$

that is,

$$2k^3C_s^2C_g^2 - 3\pi Gk^2(\mu_gC_s^2 + \mu_sC_g^2) + k\kappa^2(C_s^2 + C_g^2) - \pi G\kappa^2(\mu_g + \mu_s) = 0\,. \quad (7)$$

We want to express equations (6) and (7) in terms of dimensionless quantities. Define $C = \pi G\mu_t/\kappa$ = unit of velocity and $\Lambda = \pi G\mu_t/\kappa^2$ = unit of wavelength. Also define:

$$k\cdot\Lambda = \chi\,, \quad \mu_g/\mu_t = \epsilon\,,$$
$$[(C_{s,\min})_{2\text{-}f}/C] = q_s\,, \quad \text{and} \quad C_g/C = q_g \quad (8)$$

Here, C is equal to $(C_{s,\min})_{1\text{-}f}$, the Toomre critical stellar velocity dispersion, for the case when all the disk density is in the stellar fluid alone. Note that $f = \mu_g/\mu_s$, the gas fraction, equals $(\epsilon/1-\epsilon)$ and $q_s = Q_s(1-\epsilon)$ and $q_g = Q_g\epsilon$, where Q_s $(= \kappa C_s/\pi G\mu_s)$ and Q_g $(= \kappa C_g/\pi G\mu_g)$ are the respective Toomre factors for the stars-alone and gas-alone systems.

Equations (6) and (7) when expressed in terms of the above set of dimensionless parameters (eq. [8]), reduce respectively to:

$$\frac{2x(1-\epsilon)}{1 + x^2q_s^2} + \frac{2x\epsilon}{1 + x^2q_g^2} = 1 \quad (9)$$

and

$$2x^3q_s^2q_g^2 - 3x^2[\epsilon q_s^2 + (1-\epsilon)q_g^2] + x(q_s^2 + q_g^2) - 1 = 0\,. \quad (10)$$

We next solve equations (9) and (10) together numerically, and obtain q_s for a given (q_g, ϵ). That is, we obtain q_s at a given set of values for κ, μ_t, $\epsilon(= \mu_g/\mu_t)$, and C_g. To check that this value of q_s does indeed leave the system stable at all x, we have to make sure that the function $\omega^2(k)$ is indeed greater than 0 for all x values between $x = 1/(1-\epsilon)$ and $1/\epsilon$. We do this by evaluating the left-hand side of equation (9) (at the above q_s value) and checking that it is less than 1 in the above x-range.

In Figure 1, we present the results for q_s, that is, $(C_{s,\min})_{2\text{-}f}/C$ as a function of μ_g/μ_s for two sets of values of κ, μ_t—each set giving rise to one of the two curves. We keep C_g constant at 5 km s^{-1} for both cases. Under this assumption, q_s is effectively a function only of f, that is, μ_g/μ_s.

From Figure 1, we see that at any μ_g/μ_s, C; $(C_{s,\min})_{2\text{-}f}$ is always greater than C $[= (C_{s,\min})_{1\text{-}f}]$; that is, it is harder to stabilize a two-fluid disk than the corresponding one-fluid stellar disk (of the same total disk surface density). Second, $(C_{s,\min})_{2\text{-}f}/C$ increases as μ_g/μ_s is increased. [Qualitatively, both these results were expected from Fig. 3 of Paper I, where we found that if a small fraction of the total density of an initially neutrally stable stellar disk is put in a cold fluid, that is, gas, the resulting two-fluid system (at the same C_s) is unstable and becomes progressively more unstable as μ_g/μ_s is increased. Hence $(C_{s,\min})_{2\text{-}f}$ would be expected to increase with increasing μ_g/μ_s at constant total disk surface density, as is indeed seen to be true from Fig. 1 here.] In the limiting

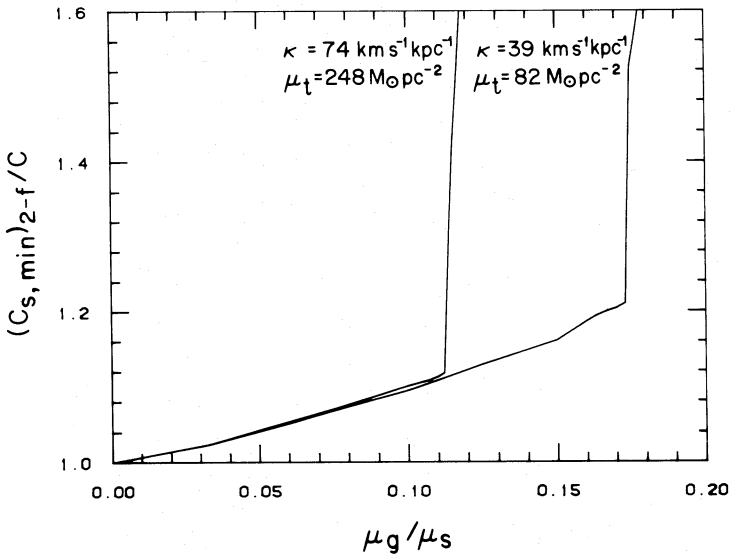

FIG. 1.—The ratio of the critical stellar velocity dispersions for a two-fluid system and a one-fluid stellar system (at constant total surface density) as a function of the gas fraction μ_g/μ_s. Two cases as shown for $\kappa = 74$ km s^{-1} kpc^{-1}, $\mu_t = 248\ M_\odot$ pc^{-2} (giving $\mu_t/\kappa = 3.3\ M_\odot$ pc^{-2}/km s^{-1} kpc^{-1}), and $\kappa = 39$ km s^{-1} kpc^{-1}, $\mu_t = 82\ M_\odot$ pc^{-2} (giving $\mu_t/\kappa = 2.1\ M_\odot$ pc^{-2}/km s^{-1} kpc^{-1}). $C_g = 5$ km s^{-1} for both cases. The divergence of $(C_{s,\min})_{2\text{-}f}/C$ occurs where the gas alone approaches neutral equilibrium ($Q_g \sim 1$).

case of $\mu_g/\mu_s \to 0$, $(C_{s,\min})_{2\text{-}f}/C$ does tend to 1 in each case, as expected.

We see that the ratio $(C_{s,\min})_{2\text{-}f}/C$ is a linearly increasing function of μ_g/μ_s, for low values of the same. At higher μ_g/μ_s, this ratio increases nonlinearly and finally diverges at very large gas fraction, μ_g/μ_s. The onset of divergence is related to the approach of $(k_0)_{2\text{-}f}$ toward $\sim(k_0)_g$—away from $\sim(k_0)_s$, which in turn is coincident with the gas-alone tending toward neutral equilibrium ($Q_g \to 1$) since the stellar contribution is negligible near $(k_0)_g$. Now, as $Q_g \to 1$, $\alpha_g \to 0$. That is,

$$\alpha_g = (\kappa^2 + k^2 C_g^{\,2} - 2\pi G k \mu_g) \to 0\ ,$$

which gives

$$\frac{2\pi G k \mu_g}{\kappa^2 + k^2 C_g^{\,2}} \to 1\ . \qquad (11)$$

Thus, at $(k_0)_{2\text{-}f} \to (k_0)_g$, equation (6), which is a necessary condition for two-fluid neutral equilibrium, can be satisfied, in view of equation (11), only by $C_s \to \infty$. The sharp increase in $(C_{s,\min})_{2\text{-}f}$ occurs at a lower μ_g/μ_s for a higher μ_t/κ, as seen from equation (11) and in Figure 1. Also, at a given μ_t/κ, the higher the value of C_g, the larger is the value of μ_g/μ_s at which this divergence occurs. For example, if $C_g = 8$ km s^{-1} were to be used in Figure 1, the divergence would occur at a gas density that is $\sim(8/5) = 1.6$ times larger.

In the limit that $\alpha_g \lesssim 0$, the two-fluid system *cannot* be stabilized—that is, equation (6) cannot be satisfied—no matter how high C_s is; hence the function $(C_{s,\min})_{2\text{-}f}$ is no longer meaningful. In fact, an effective upper limit on $(C_{s,\min})_{2\text{-}f}$ may be placed as the case when $(C_{s,\min})_{2\text{-}f}$ is a significant fraction of the rotational velocity, since the system cannot be treated as a disk any more.

b) Numerical Evaluation of $(C_{s,\min})_{2\text{-}f}$, and the Characteristics of $(C_{s,\min})_{2\text{-}f}$ in the Galaxy

Here we consider the most general form of ω^2 as applicable to a two-fluid system in a finite height disk (eq. [23] of Paper I). The quantities $2h_s$ and $2h_g$ are the total scale heights for the stars and the gas, respectively. In this case, equations similar to (9) and (10) may be derived but would be tedious to solve analytically. Hence, instead, for a given set of values for the parameters κ, μ_s, μ_g, C_g, h_g, we obtain $(C_{s,\min})_{2\text{-}f}$ by maximizing $\omega^2(k)$ (eq. [23], Paper I) with respect to k for different C_s, and the C_s for which the peak in ω^2 equals zero is then critical stellar velocity dispersion, $(C_{s,\min})_{2\text{-}f}$. We determine h_s using equation (28) of Paper I, $n = 2$ (see § III*a*, Paper I).

For comparison, we employ a similar procedure (beginning with eq. [25], § II*d*, Paper I) to obtain $(C_{s,\min})_{1\text{-}f}$ for a finite height disk. Here h_s is obtained using equation (28), $n = 1$ (see III*a*, Paper I).

In Figure 2, we present results for $(C_{s,\min})_{2\text{-}f}$ as a function of R, the galactocentric radius for $\mu_g/\mu_s = 0.1$, 0.15, and 0.2. $R = 10$ kpc denotes the solar neighborhood. For the galactic disk, κ and μ_t are taken from Caldwell and Ostriker (1981). We assume $\mu_g = \mu_t - \mu_s$. The input data and results for Figure 2 as well as the corresponding $(C_{s,\min})_{1\text{-}f}$ at each R are listed in Table 1. The numerical results (for a finite height disk) agree very well with the analytical results (for an infinitesimally thin disk) given in § II*a*: The difference [in each $(C_{s,\min})_{2\text{-}f}$ and $(C_{s,\min})_{1\text{-}f}$] is less than 10% as long as

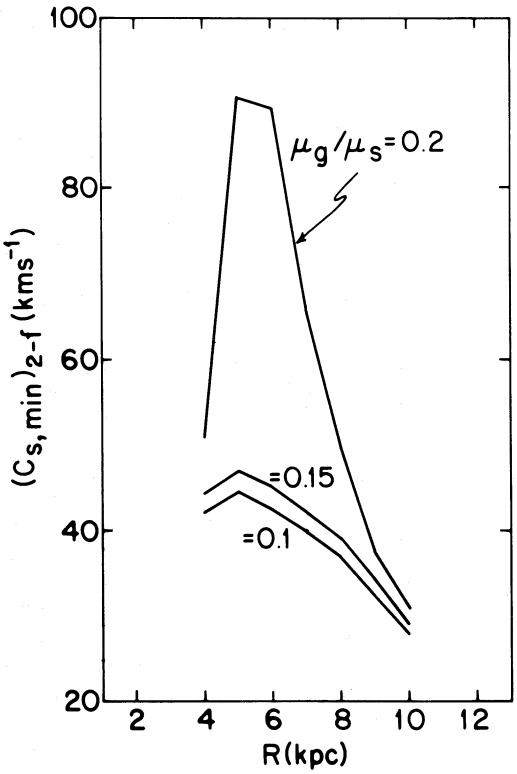

FIG. 2.—$(C_{s,\min})_{2\text{-}f}$, the two-fluid critical stellar velocity dispersion versus R, the galactocentric radius. The input parameters, κ, μ_t, as functions of R, are listed in Table 1. The peak in $(C_{s,\min})_{2\text{-}f}$ vs. R (for a constant μ_g/μ_s with R) occurs at the peak in μ_t/κ vs. R; that is, at $R = 5$ kpc. The location of the peak coincides with the molecular "ring" in the Galaxy.

TABLE 1

$(C_{s,\min})_{2\text{-}f}$ AS A FUNCTION OF R IN THE GALAXY

			$\mu_g/\mu_s = 0.1$		$\mu_g/\mu_s = 0.15$		$\mu_g/\mu_s = 0.2$		
R (kpc)	κ[a] (km s^{-1} kpc^{-1})	μ_t[a] ($M_\odot$ pc^{-2})	$(C_{s,\min})_{2\text{-}f}$ (km s^{-1})	$\frac{(C_{s,\min})_{2\text{-}f}}{(C_{s,\min})_{1\text{-}f}}$	$(C_{s,\min})_{2\text{-}f}$ (km s^{-1})	$\frac{(C_{s,\min})_{2\text{-}f}}{(C_{s,\min})_{1\text{-}f}}$	$(C_{s,\min})_{2\text{-}f}$ (km s^{-1})	$\frac{(C_{s,\min})_{2\text{-}f}}{(C_{s,\min})_{1\text{-}f}}$	$(C_{s,\min})_{1\text{-}f}$[b] (km s^{-1})
4	89	281	42.0	1.15	44.4	1.22	50.8	1.39	36.4
5	74	248	44.5	1.11	47.1	1.18	90.5	2.26	39.9
6	65	209	42.6	1.09	45.3	1.16	89.3	2.29	39.0
7	57	171	39.8	1.11	42.3	1.18	65.6	1.83	35.8
8	49	137	36.9	1.11	38.9	1.17	50.0	1.51	33.0
9	44	107	32.3	1.10	34.3	1.17	37.7	1.29	29.2
10	39	82	27.8	1.10	29.1	1.15	31.0	1.23	25.2

[a] The values of κ and μ_t are adapted from Caldwell and Ostriker 1981.

[b] $(C_{s,\min})_{1\text{-}f}$ is evaluated numerically for a finite height stellar disk with $(\mu_s)_{1\text{-}f} = (\mu_t)_{2\text{-}f}$.

$(k_0)_{2\text{-}f} \sim (k_0)_s$, that is, at low μ_g/μ_s, and is $\lesssim 30\%$ when $(k_0)_{2\text{-}f} \to (k_0)_g$, that is, at high μ_g/μ_s. Thus the value of μ_g/μ_s at which the onset of divergence in Figure 1 occurs is underestimated slightly.

From Figure 2, we see that at a given R, $(C_{s,\min})_{2\text{-}f}$ is higher for a higher μ_g/μ_s; and at a given μ_g/μ_s, the highest $(C_{s,\min})_{2\text{-}f}$ coincides with the position of highest μ_t/κ (as seen from Table 1). Also, note that, at a given μ_g/μ_s, $(C_{s,\min})_{2\text{-}f}$ as a function of R peaks at an intermediate point ($R = 5$ kpc) in the galactic disk.

Now it is most difficult (that is, it takes the longest time) to establish two-fluid neutral equilibrium in the region where $(C_{s,\min})_{2\text{-}f}$ peaks. Therefore, the two-fluid instabilities and, in view of the large μ_g/κ in the region where $(C_{s,\min})_{2\text{-}f}$ peaks, the induced gas instabilities as well (discussed in § III) are more likely to occur in this region. The formation of gravitational instabilities will lead to a significant increase in the gas density which will result in the formation of dense clouds or cloud complexes and a consequent conversion of hydrogen to molecular form. The molecular to atomic surface density ratio in the ISM, $\mu_g(H_2)/\mu_g(H\ I)$, will therefore peak in the same region where $(C_{s,\min})_{2\text{-}f}(R)$ peaks. Note that this result arises solely due to the interaction between the two fluids in the two-fluid scheme. Conversely, when the disk is treated as consisting of two separate noninteracting fluids, there is no connection expected between the stellar velocity dispersion and the form of density in the gas.

Given the particular values for $\kappa(R)$, $\mu_t(R)$ in the Galaxy (and assuming a constant μ_g/μ_s at all R), we predict that the maximum gas fraction in the molecular form will be found to occur at $R \approx 5$ kpc, which does indeed coincide with the peak (in density) of the "molecular ring" (Scoville and Solomon 1975) in the Galaxy, thus corroborating the above discussion. The analysis in this section can also be applied to external galaxies, and we plan to do this in a future paper.

A comment is in order about the uncertainty in the absolute value of $(C_{s,\min})_{2\text{-}f}$ resulting from the same in μ_g/μ_s and μ_t in the disk. Observations of gas density in the disk indicate (see § III*a* of Paper I) that over $R = 4$–10 kpc, μ_g/μ_t is expected to be ~ 0.1–0.15 (see Sanders, Solomon, and Scoville 1984). But μ_g is uncertain by $\sim 50\%$ and μ_t is known only from approximate exponential (galactic mass) models (see discussion in § III*a* of Paper I). Therefore, there is a considerable range (see Table 1) in the predicted values of $(C_{s,\min})_{2\text{-}f}$ at each R in the Galaxy. There exists a further (and more important) uncertainty in $(C_{s,\min})_{2\text{-}f}$, however, as explained next. Now, the results for $(C_{s,\min})_{2\text{-}f}$ given in Table 1 represent the case when all the nongaseous disk density—that is, $(\mu_t - \mu_g)$—is in a single stellar component characterized by $(C_{s,\min})_{2\text{-}f}$. In the solar neighborhood, however, only a fraction of the nongaseous disk density is accounted for by the observed disk stars. If the remaining density resides in a higher velocity component, then the value of $(C_{s,\min})_{2\text{-}f}$ for disk stability at $R = 10$ kpc as derived above is overestimated. Indeed, Nakamura (1978)[5] has done the technically identical analysis of two-fluid neutral equilibrium except from the point of view of determining only a lower limit on the velocity of the as yet unseen disk component in the solar neighborhood. Nakamura, assuming gas to be stable, estimates this to be 25 km s^{-1} which is roughly equal to the two-fluid critical stellar velocity dispersion at $R = 10$ kpc, with $\mu_g/\mu_s = 0.1$ (see Table 1). One cannot, however, *a priori* do a similar study for the nonlocal regions. For these cases as well as for $R = 10$ kpc, we assume that all the nongaseous disk density is in a single stellar component. Under this assumption, the values of $(C_{s,\min})_{2\text{-}f}$ that we have derived (Table 1) are correct.

We end this section by a brief discussion about the comparison of the current observed C_s in the disk with $(C_{s,\min})_{2\text{-}f}$, calculated above. For a one-fluid stellar disk, Toomre (1964) argued that even an initially unstable (one-fluid) disk would undergo several successive generations of instabilities, each of which would add some more kinetic energy of random motions to the system. In a few rotation periods, the system would then reach an equilibrium state in which the random velocity at each point in the Galaxy would have become about equal to the local $(C_{s,\min})_{1\text{-}f}$, that is, the minimum value needed for disk stability at each point.

From the various cases considered for a two-fluid system (see § III*b* of Paper I), we found that a typical two-fluid instability has a time growth, $T_e \approx$ a few $\times 10^7$ years ($\ll$ the age of the Galaxy). Therefore, we propose that prior to some unspecified earlier epoch, the Galaxy must have been unstable and then reached two-fluid neutral equilibrium; with the stellar velocity dispersion at each point $\sim (C_{s,\min})_{2\text{-}f}$. We expect, then,

[5] This paper by Nakamura was recently brought to our attention, after we had completed our work presented in this paper.

that at the current epoch the stellar velocity dispersion, on average, at any point in the disk (for a uniform disk) equals or exceeds the local value of $(C_{s,\min})_{2\text{-}f}$. This increase in C_s above and beyond $(C_{s,\min})_{2\text{-}f}$, which may be attributed to an acceleration mechanism such as the Spitzer–Schwarzschild (1953) mechanism, would not disturb the disk stability.

The higher value of $(C_{s,\min})_{2\text{-}f}$ as compared to $(C_{s,\min})_{1\text{-}f}$ means that during the evolution of the disk, it is harder to stabilize a two-fluid disk. Once the disk is stabilized, however, the two-fluid scheme gives a higher value for the lower limit on the observed stellar velocity dispersion in a disk at the current epoch than the one given by the Toomre model for a one-fluid stellar disk.

III. GAS INSTABILITIES INDUCED BY THE TWO-FLUID INSTABILITIES

As discussed earlier in § I of Paper I, over a large region in the inner Galaxy the gas is on the brink of allowing the growth of gravitational instabilities, requiring an increase in the overall gas density by only a factor of 2 or less before the gas alone becomes unstable to the growth of gravitational instabilities. In this section, we investigate whether the increase in the gas density (for gas within a two-fluid instability), resulting from the growth of a two-fluid instability, can precipitate the formation of instabilities in the gas alone or not. In § III*a*, we calculate the gas density amplification resulting due to the growth of a two-fluid instability. In § III*b*, we derive the criterion for the onset of induced gas instabilities, and in § III*c* we study the properties of the induced gas instabilities in the Galaxy.

a) Gas Density Amplification Due to a Two-Fluid Instability

The increase in gas density resulting from the growth of a two-fluid instability depends on the relative fractional growth in the perturbations in the two fluids, that is, on $(\delta\mu_g/\mu_{g0})/(\delta\mu_s/\mu_{s0})$, where μ_{g0} and μ_{s0} are the unperturbed gas and stellar surface densities respectively, and on the maximum allowed fractional growth in the stellar fluid perturbation which is given by $(\delta\mu_s/\mu_{s0}) \approx 1$. The latter condition arises from our assumption that the two-fluid instabilities can continue to grow only as long as the stellar fluid is far from the nonlinear regime, the reason being that the stellar fluid cannot dissipate the increase in the random motion "pressure" due to the increase in the density, whereas the gas can dissipate the heat of compression via collision, radiation, turbulence etc.

Now, although a perturbation (k, ω) to the two-fluid system grows at the same rate in both the fluids since ω is the same, the perturbation does not become nonlinear at the same epoch in both the fluids, as shown next. This is because, as shown in § III*e* of Paper I, the original magnitudes of the perturbation surface densities, $\delta\mu_g'$ and $\delta\mu_s'$, are not independent for a two-fluid case; rather, they are governed by the coupling of the two fluids that occurs via the force equation. The velocity dispersion of either isothermal fluid dictates its response to the joint gravitational perturbation (see eqs. [33] and [34] of Paper I). Equation (35) from Paper I gives:

$$\frac{(\delta\mu_g'/\mu_{g0})}{(\delta\mu_s'/\mu_{s0})} = \frac{\kappa^2 + k^2C_s^2 - \omega^2}{\kappa^2 + k^2C_g^2 - \omega^2} . \tag{12}$$

Since we are considering two-fluid instabilities, $\omega^2(k) < 0$ in the last three equations and hence the ratio in equation (12) is a positive definite quantity. Starting from $t = 0$, consider the ratio of the fractional growth in the perturbation surface density for the two fluids, at a given time t later:

$$\frac{(\delta\mu_g/\mu_{g0})}{(\delta\mu_s/\mu_{s0})} = \frac{\kappa^2 + k^2C_s^2 - \omega^2}{\kappa^2 + k^2C_g^2 - \omega^2} . \tag{13}$$

Since the maximum allowed value for $(\delta\mu_s/\mu_{s0})$ is ~ 1, we find from equation (13) that the corresponding value of $\delta\mu_g/\mu_{g0}$ allowed is:

$$(\delta\mu_g/\mu_{g0})\Big|_{(\delta\mu_s/\mu_{s0})=1} = \frac{(\kappa^2 + k^2C_s^2 - \omega^2)}{(\kappa^2 + k^2C_g^2 - \omega^2)} . \tag{14}$$

This quantity is greater than 1 when $C_s > C_g$. We denfie A, the gas amplification factor, as:

$$A = \left[1 + \left(\frac{\kappa^2 + k^2C_s^2 - \omega^2}{\kappa^2 + k^2C_g^2 - \omega^2}\right)\right] . \tag{15}$$

Thus $\mu_{g0} \cdot A$ is the gas density reached as a result of the growth of a given two-fluid instability (k, ω). Note that $A > 2$; that is, the gas is in a nonlinear regime. We assume that the gas continues its collapse even after reaching the nonlinear density; hence we can apply equation (13), derived from a linear calculation, to the gas in a nonlinear regime.

Conversely, for a given set of values for the input parameters and $\delta\mu_g/\mu_{g0}$, we can, using equation (13), determine $\delta\mu_s/\mu_{s0}$. The maximum value of the latter is 1 for a constant set of input parameters, especially C_s. Note that because the stellar fluid is incompressible, its subsequent separate collapse (unlike that of gas to be studied next) is not expected to take place. Instead we expect the density enhancement in the stellar fluid to disperse with time. Hence the above calculated value of $\delta\mu_s/\mu_{s0}$ is applicable only for the young $(t \lesssim t_{2\text{-}f} = 1/\omega_{2\text{-}f})$ two-fluid instabilities.

b) Criterion for the Onset of Induced Gas Instabilities

The one-fluid gas dispersion relation for a finite height disk is given (by eq. [26] of Paper I) as:

$$\omega^2{}_{1\text{-}f} = \kappa^2 + k^2C_g^2 - 2\pi Gk\mu_{g0}\{[1 - \exp(-kh_g)]/kh_g\} . \tag{16}$$

With $(\mu_{g0}\, A)$ as the effective gas density, resulting from the growth of a two-fluid instability, the above equation reduces to

$$\omega^2{}_{1\text{-}f} = \kappa^2 + k^2C_g^2 - 2\pi Gk(\mu_{g0}\, A)\{[1 - \exp(-kh_g)]/kh_g\} . \tag{17}$$

Because of the compressible nature of the gas, the value of C_g is unaltered even after μ_g increases. Equation (17) is applicable to all k values larger than the one characterizing the particular two-fluid instability under consideration.

From equation (16), we can numerically obtain $(\mu_g)_{\text{critical}}$, the critical gas density (at a given C_g) for which gas-alone instabilities can occur. [Note that at $(\mu_g)_{\text{critical}}$, Q_g (for a finite height gas disk) equals 1.] Comparing equations (16) and (17), it is clear that even when the average observed gas density, μ_{g0}, is less than $(\mu_g)_{\text{critical}}$, the (induced) gas instabilities can still occur if $\mu_{g0} > [(\mu_g)_{\text{critical}}/A]$, hence the label "induced" for these instabilities. $\omega^2{}_{1\text{-}f}(k)$ (as given by eq. [17]) < 0 constitutes the criterion for the onset of induced gas

instabilities. Thus, $(\mu_g)_{\rm critical}$ has been effectively redefined by taking account of the gas amplification resulting from the growth of a two-fluid instability. Therefore, while considering the stability of the gas in a two-fluid system, one cannot treat the gas separately as an isolated system. As a result of the compressible nature of the gas, once it becomes unstable and the density increases, most of the gas may be converted to a molecular form. Thus the stability as well as the form of the gas in a two-fluid system is affected by the stellar fluid in the system.

c) *Results for Induced Gas Instabilities*

The analysis for induced gas instabilities is applicable to a section of a real galaxy only when the local value of C_s is less than $(C_{s,\rm min})_{2\text{-}f}$. If the gas does become unstable, its further evolution could only be studied by doing a nonlinear analysis which we do not attempt to do in this paper. However, if such induced gas instabilities were feasible and if the resulting instabilities were long-lived ($\gg t_{\rm free\text{-}fall}$), as there is evidence for from the observations of a dense interstellar medium in the Galaxy, then we could explain the existence of dense gas clouds in the ISM formed by gravitational instabilities [with μ_g in clouds $\gg(\mu_g)_{\rm critical}$] even when the average gas density μ_g ($=\mu_{g0}$) in ISM is $<(\mu_g)_{\rm critical}$.

For the purpose of illustrating the properties of the resulting typical induced gas instabilities, we consider the following hypothetical cases. Assuming that C_s at each point is an arbitrary fraction, δ (which is constant for all R), of the local $(C_{s,\rm min})_{2\text{-}f}$, we first calculate the local value of A and hence the effective gas density $(\mu_g)_{\rm effective}=\mu_{g0}A$, at each R. For this, we use $(C_{s,\rm min})_{2\text{-}f}$ as a function of R as given in Table 1 and use equation (23) of Paper I to derive $\omega^2{}_{2\text{-}f}$. Next, we calculate the characteristics, $k_{\rm peak}$ and $\omega_{\rm peak}$, for the respective fastest growing mode for the gas-alone system at $\mu_g=(\mu_g)_{\rm effective}$. We carry out this entire procedure first for $\delta=0.8$ and then repeat it for $\delta=0.9$ so as to study the variation (if any) in the properties of the resulting induced gas instabilities. The results from this calculation are given in Table 2. At each R in each case, we find that A, the gas amplification factor, is typically in the range of 3.5 to 4 (and is therefore moderately independent of the variation in C_s). The induced gas instabilities on the other hand are more likely (as seen from values of $(\mu_g)_{\rm effective}/(\mu_g)_{\rm critical}$, Table 2) in the intermediate region in the galaxy, from $R=4$ to 7 kpc, that is, where μ_g/κ is high (low Q_g). Although this ratio is greater than 1 for each R, the actual likelihood of induced gas instabilities at each R must depend on the respective peak growth rate which is seen to be maximum in the intermediate R-range.

Note that we have assumed a constant value of $\mu_g/\mu_s(=0.1)$ in doing the above calculations, so that μ_g peaks at the lowest R ($\sim$4 kpc) under consideration here. Hence, the resulting coincidence between the region of fast growth of the induced gas instabilities and the observed "ring" region of the molecular gas density distribution is not simply due to the high total gas density.

The location of the peak in $(C_{s,\rm min})_{2\text{-}f}$ coincides with the

TABLE 2A[a]

RESULTS FOR INDUCED GAS INSTABILITIES

R (kpc)	C_s (km s^{-1})	μ_{g0}[b] ($M_\odot$ pc^{-2})	$(\mu_g)_{\rm critical}$ ($M_\odot$ pc^{-2})	Gas Amplification Factor A	$\frac{(\mu_g)_{\rm effective}}{(\mu_g)_{\rm critical}}$	$(\lambda_{1\text{-}f})^{-1}$ (kpc^{-1})	$(\omega^2{}_{1\text{-}f})_{\rm peak}$ (km s^{-1} kpc^{-1})^2	$M_{\rm gas}$ (in induced gas instabilities) ($M_\odot$)
4	33.6	25.5	32.8	3.60	2.80	2.42	8.83×10^3	1.51×10^7
5	35.6	22.5	27.5	3.80	3.11	2.39	9.65×10^3	1.34×10^7
6	34.1	19.0	24.1	3.83	3.02	2.21	7.89×10^3	1.49×10^7
7	31.8	15.5	21.1	3.74	2.75	1.97	5.57×10^3	1.49×10^7
8	29.5	12.5	18.3	3.73	2.55	1.75	3.97×10^3	1.52×10^7
9	25.8	9.7	16.1	3.58	2.16	1.48	2.23×10^3	1.59×10^7
10	22.2	7.5	14.4	3.41	1.78	1.23	1.05×10^3	1.69×10^7

[a] Case *a*: $C_s=0.8\,(C_{s,\rm min})_{2\text{-}f}$. The values of $(C_{s,\rm min})_{2\text{-}f}$ are taken for case $\mu_g/\mu_s=0.1$ from Table 1.
[b] $\mu_{g0}=0.1\mu_{s0}$. $\mu_t(=\mu_{g0}+\mu_{s0})$ is adopted from Caldwell and Ostriker 1981.

TABLE 2B[a]

RESULTS FOR INDUCED GAS INSTABILITIES

R (kpc)	C_s (km s^{-1})	μ_{g0}[b] ($M_\odot$ pc^{-2})	$(\mu_g)_{\rm critical}$ ($M_\odot$ pc^{-2})	Gas Amplification Factor A	$\frac{(\mu_g)_{\rm effective}}{(\mu_g)_{\rm critical}}$	$(\lambda_{1\text{-}f})^{-1}$ (kpc)$^{-1}$	$(\omega^2{}_{1\text{-}f})_{\rm peak}$ (km s^{-1} kpc^{-1})^2	$M_{\rm gas}$ (in induced gas instabilities) ($M_\odot$)
4	37.8	25.5	32.8	3.27	2.54	2.36	6.82×10^3	1.50×10^7
5	40.1	22.5	27.5	3.34	2.73	2.24	7.17×10^3	1.50×10^7
6	38.3	19.0	24.1	3.32	2.62	2.06	5.68×10^3	1.49×10^7
7	35.8	15.5	21.2	3.35	2.46	1.86	4.27×10^3	1.50×10^7
8	33.2	12.5	18.3	3.35	2.26	1.65	3.03×10^3	1.54×10^7
9	29.1	9.7	16.1	3.33	1.94	1.40	1.63×10^3	1.60×10^7
10	25.0	7.5	14.4	3.18	1.66	1.18	7.79×10^2	1.71×10^7

[a] Case *b*: $C_s=0.9\times(C_{s,\rm min})_{2\text{-}f}$. The values of $(C_{s,\rm min})_{2\text{-}f}$ are taken for case $\mu_g/\mu_s=0.1$ from Table 1.
[b] $\mu_{g0}=0.1\mu_{s0}$; $\mu_t(=\mu_{g0}+\mu_{s0})$ is adopted from Caldwell and Ostriker 1981.

region of maximum likelihood of induced gas instabilities. This is because both of these functions are increasing functions of μ_t/κ at a constant μ_g/μ_s. If μ_g/μ_s were to change with R so that μ_t/κ and μ_g/κ were to peak at different R values, the above two functions need not peak at the same location in the Galaxy.

The wavelength for a typical induced gas instability is $\sim$400–500 pc, and the mass of gas in such a typical instability at any R is ~ 1–$2 \times 10^7\ M_\odot$ (see Tables 2A and 2B). Since we have not considered the nonlinear case, the actual scale of the resulting inhomogeneity may be substantially less, but the mass will be preserved. Each of these features may very well be the clusters of molecular clouds seen by Sanders and Solomon (1984). Recall from Paper I, § III*b*, that the wavelength for a typical two-fluid instability in the Galaxy is $\sim$2–3 kpc and the mass of gas in it is $\sim 4 \times 10^7$–$10^8\ M_\odot$. Therefore, when induced gas instabilities do occur, there are typically from five to seven regions, each separated by about 500 pc within a typical two-fluid instability, assuming that all the gas in the two-fluid instability ends up in such condensations and that consequent fragmentation (if any) does not destroy a given clump totally.

In § III*a*, we saw that as a result of the onset of a two-fluid instability, while μ_s increases to $2\mu_{s0}$, μ_g increases to $(\mu_g)_{\text{effective}} = \mu_{g0} A$ at the same time. Hence, the typical linear extent of the region occupied by the stellar component and the gaseous component within a two-fluid instability consequent to the growth in density due to the two-fluid instability of wavelength $\lambda_{2\text{-}f}$ is $\lambda_{2\text{-}f}/2^{1/2}$ and $\lambda_{2\text{-}f}/[A]^{1/2}$, respectively. Pictorially, the spatial distribution of these various regions may be schematically illustrated as in Figure 3.

IV. DISCUSSION OF THE SCALE-LENGTH OF THE (NONAXISYMMETRIC) TWO-FLUID INSTABILITIES AND THE SPIRAL STRUCTURE IN A DISK

In this paper (and in Paper I), we consider only the axisymmetric case (for the perturbations to the two-fluid system). Now for a two-dimensional disk, the most general perturbation is nonaxisymmetric, and the treatment of this is not a simple extension of the axisymmetric analysis in the case of a differentially rotating disk. We plan to carry out two-fluid nonaxisymmetric analysis in a future paper. The nonaxisymmetric two-fluid instabilities in a differentially rotating galactic disk can potentially explain the spiral features in disk galaxies, consisting of stars and gas.

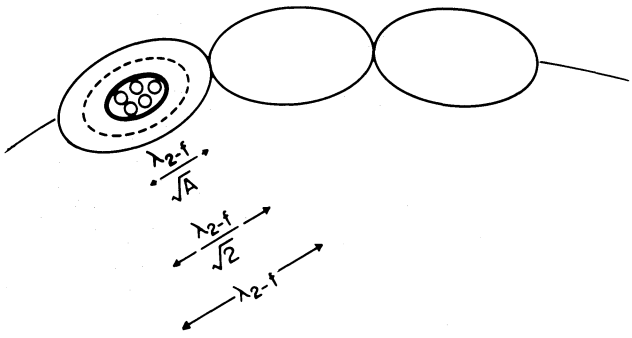

FIG. 3.—Schematic drawing of the various regions within a two-fluid instability. Each of the three outer solid curves represents a two-fluid instability of wavelength, $\lambda_{2\text{-}f} \sim 2$–3 kpc. The stellar and the gas components, consequent to the growth in density due to the two-fluid instability, lie within areas bound by the dashed curve and the dark solid curve, respectively, within each instability; this has been shown explicitly in the leftmost section. The surface areas of these two regions are given by $(\lambda_{2\text{-}f})^2/2$ and $(\lambda_{2\text{-}f})^2/A$ respectively, where $A \sim 3.5$ is the gas amplification factor. The clumps within the area occupied by the gas at high density are the induced gas instabilities, each a few hundred parsecs in extent.

Observationally, it is seen that very few spiral galaxies exhibit a grand two-arm or three-arm spiral pattern, and most galaxies contain a messy distribution of spiral features on a smaller scale, $\sim$2–3 kpc (Sandage 1961; Prendergast 1967; Goldreich and Lynden-Bell 1965; Toomre 1977; Elmegreen and Elmegreen 1982). The two-fluid instabilities, especially in the nonaxisymmetric case, may represent the spiral arm segments or features, each of typical wavelength $\sim$2–3 kpc, seen in spiral galaxies. We view the spiral features in spiral galaxies not as quasi-stationary wave phenomena (unlike in the density wave theory; see Lin and Shu 1964, 1966) but rather as material arms, that is, as randomly occurring, sheared two-fluid gravitational instabilities. In the past, Goldreich and Lynden-Bell (1965) have proposed that spiral arms (in Sc galaxies) be considered as sheared gravitational instabilities. Toomre (1977) also has stressed the idea that the "secondary" spiral features may be considered to be material arms. Both Goldreich and Lynden-Bell (1965) and Toomre (1964), however, deal with a one-fluid stellar disk, and the wavelength obtained is too large ($\sim$5–8 kpc) (Toomre 1964) to represent a typical (small-scale) spiral feature in a galaxy, as was pointed out by Toomre. The addition of the gas in our two-fluid treatment reduces the wavelength, bringing it into closer agreement with the observations.

At the end, we note that this alternative point of view—namely, that the spiral arms are material entities—cannot explain the grand spiral pattern seen in some external galaxies (such as M81, M51 [Sandage 1961]). The grand spiral pattern, when present, could be driven by a companion galaxy (Toomre 1969) or by a central bar (Toomre 1969; Sanders and Huntley 1976; Feldman and Lin 1973).

It may well be that for isolated, non-barred, gas-rich galaxies, the two-fluid instabilities dominantly determine the spiral structure, while for the galaxies that do exhibit grand spiral pattern, the density wave theory or any other theory describing the spiral pattern as a wave phenomenon may be important. Even in the latter cases, however, there will still be random and localized perturbations (on the underlying grand spiral pattern) that may be due to the two-fluid instabilities.

V. CONCLUSIONS

The conclusions from this paper are summarized below:

1. The critical stellar velocity dispersion required for the disk stability is significantly larger for the two-fluid system than it is for the one-fluid stellar system (of same total disk surface density), even when only a small fraction (0.1–0.2) of the total disk density is in a cold fluid (that is, gas). Therefore, it is harder to stabilize a two-fluid disk than the corresponding one-fluid stellar disk. The observed stellar velocity dispersion should exceed the two-fluid value (on average) for a stable galaxy.

$(C_{s,\min})_{2\text{-}f}$ is an increasing function of μ_g/μ_s and μ_t/κ. In the Galaxy, $(C_{s,\min})_{2\text{-}f}$ as a function of R peaks when μ_t/κ peaks, at galactocentric radii of $R \sim 5$–7 kpc; two-fluid instabilities are most likely to occur in this region. We expect

that gravitational instabilities lead to the formation of giant molecular clouds through two-fluid instabilities and subsequent induced gas instabilities. Observations of the distribution of dense interstellar matter (giant molecular clouds) show a maximum concentration in a "ring" between 5 and 8 kpc (see, e.g., Sanders, Solomon, and Scoville 1984), in good agreement with the above result.

2. At the increased gas density resulting from the growth of a two-fluid instability, the gas itself may become unstable to the growth of gravitational perturbations, thus resulting in the formation of induced gas instabilities, even when originally the gas by itself is stable.

We find that the growth rate for induced gas instabilities is greater in the regions of high μ_g/κ—that is, in the intermediate region ($R = 4$–7 kpc) in the Galaxy. The typical wavelength of an induced gas instability in the Galaxy is $\sim$400–500 pc. Each of these contains gas of total mass ~ 1–$2 \times 10^7\ M_\odot$. Such inhomogeneities may be identified with the observational feature of clusters of giant molecular clouds (Sanders and Solomon 1984).

We can thus explain the existence of dense, molecular gas clouds in the ISM even when the average spread-out gas density in the ISM at the current epoch does not allow gas-alone to be unstable. Thus, the stability as well as the form of the gas in a two-fluid disk may be significantly affected by the stars in the disk.

3. The two-fluid instabilities, especially in the nonaxisymmetric case (to be presented in a future paper), may represent the spiral arm segments or features, each of typical wavelengths $\sim$2–3 kpc. We view many of the spiral features in spiral galaxies as material arms—that is, as randomly occurring, sheared two-fluid gravitational instabilities. For isolated, nonbarred, gas-rich galaxies the two-fluid instabilities may determine the spiral structure seen.

The general analysis presented here is valid for any disk galaxy. In a future paper we plan to apply the two-fluid analysis to external galaxies, so as to evaluate the stellar velocity structure and the distribution within a galaxy of the molecular gas.

We would like to thank J. P. Ostriker, D. Lynden-Bell, and S. M. Fall for useful conversations during the course of this work. Part of this work was carried out while one of us (P. S.) was a Visiting Scientist at the Institute of Astronomy, Cambridge, England, and we are grateful for the hospitality of the Institute and its Director, M. Rees.

REFERENCES

Caldwell, J. A. R., and Ostriker, J. P. 1981, *Ap. J.*, **251**, 61.
Elmegreen, D. M., and Elmegreen, B. G. 1982, *M.N.R.A.S.*, **201**, 1021.
Feldman, S. I., and Lin, C. C. 1973, *Stud. Appl. Math.*, **3**, 1.
Goldreich, P., and Lynden-Bell, D. 1965, *M.N.R.A.S.*, **130**, 125.
Jog, C. J., and Solomon, P. M. 1984, *Ap. J.*, **276**, 114 (Paper I).
Lin, C. C., and Shu, F. H. 1964, *Ap. J.*, **140**, 646.
———. 1966, *Proc. Nat. Acad. Sci.*, **55**, 229.
Nakamura, T. 1978, *Prog. Theoret. Phys.*, **59**, No. 4, 1129.
Prendergast, K. H. 1967, in *IAU Symposium No. 31, Radio Astronomy and the Galactic Systems*, ed. H. van Woerden (Dordrecht: Reidel), p. 303.
Sandage, A. 1961, *The Hubble Atlas of Galaxies* (Washington: Carnegie Institute of Washington).
Sanders, R. H., and Huntley, J. M. 1976, *Ap. J.*, **209**, 53.
Sanders, D. B., and Solomon, P. M. 1984, in preparation.
Sanders, D. B., Solomon, P. M., and Scoville, N. Z. 1984, *Ap. J.*, **276**, 182.
Scoville, N. Z., and Solomon, P. M. 1975, *Ap. J. (Letters)*, **199**, L105.
Spitzer, L., and Schwarschild, M. 1953, *Ap. J.*, **118**, 106.
Toomre, A. 1964, *Ap. J.*, **139**, 1217.
———. 1969, *Ap. J.*, **158**, 899.
———. 1977, *Ann. Rev. Astr. Ap.*, **15**, 437.

CHANDA J. JOG: Princeton University Observatory, Peyton Hall, Princeton, NJ 08544

P. M. SOLOMON: Astronomy Program, State University of New York at Stony Brook, Stony Brook, NY 11794